Band-structure-dependent transport and impact ionization in GaAs

H. Shichijo and K. Hess
Department of Electrical Engineering and Coordinated Science Laboratory, University of Illinois at Urbana-Champaign, Urbana, Illinois 61801
(Received 14 October 1980)

We have performed a Monte Carlo simulation of high-field transport in GaAs including a realistic band structure to study the band-structure dependence of electron transport and impact ionization. The band structure has been calculated using the empirical pseudopotential method. Unlike previous theories of impact ionization, our method is capable of calculating various parameters, such as mean free path, from first principles. The calculated electron mean free path, drift velocity, and impact ionization rate are in reasonable agreement with the experimental data in spite of several simplifications of the model. Within statistical uncertainty we do not observe any orientation dependence of the ionization rate in contradiction to the interpretation of recently reported experimental results. We also find that the contribution of ballistic electrons to impact ionization is negligibly small. Based on the results of the calculation, a general discussion of impact ionization is given.

I. INTRODUCTION

A large number of semiconductor devices operate on the basis of highly energetic (hot) electrons. Impact ionization is an essential mechanism in the operation of photodetectors[1] and impact-avalanche transit-time (IMPATT) diodes.[2] At present, however, the understanding of this effect is limited to a number of theories[3–8] which contain several adjustable parameters whose physical significance is not well understood. The most widely used theory of impact ionization has been given by Baraff.[5] The adjustable parameters of his theory are the threshold energy for ionization, the optical-phonon energy, the ionization mean free path, and the mean free path for optical-phonon scattering. Although some attempts have previously been made to determine these parameters theoretically,[9,10] a "complete" theory of impact ionization, which is capable of calculating these quantities (and therefore the ionization rate) from first principles, has not been developed. The main reason is that any theory applicable at extremely high electric fields (causing ionization) must abandon the effective-mass approximation or simple extensions using the $\vec{k}\cdot\vec{p}$ method, and instead include a realistic band structure. The surprising success of Baraff's theory in explaining the electric field dependence of the ionization rate is due to the adjustable parameters, which can "absorb" the band-structure effects. The inclusion of the band structure in solutions of the Boltzmann equation, however, is impractical. It is also difficult to include realistic scattering mechanisms. For example, the inclusion of both small angle scattering and randomizing scattering mechanisms in the same analytical framework is difficult. As a consequence all the previous theories are only applicable to specific materials. For instance, Dumke's theory[7] is only applicable to InSb or InAs, whereas Baraff's[5] or the Chwang *et al.*[8] treatment is only valid for nonpolar materials, such as Si or Ge.

The Monte Carlo method provides an alternative to the solution of the Boltzmann equation.[11,12] The method can take into account a large variety of scattering mechanisms, and therefore, is applicable to both polar and nonpolar semiconductors. It can calculate the quantities of interest such as drift velocity, mean free path, and average electron energy without any *a priori* assumption on the form of the distribution function. Some attempts have previously been made to calculate the impact ionization rate by the Monte Carlo method,[13,14] but without including a realistic band structure. In this paper we describe a Monte Carlo method that includes a realistic band structure as calculated by the empirical pseudopotential method.[15] This method should provide a tool for understanding electronic transport in very high fields. Of course, we do not yet have all the necessary information to perform a rigorous calculation at such high fields. For example, not much is known about the selection rules for scattering at points of low symmetry, the changes of the ionization matrix, and the scattering rate at high energies. Because of this lack of information, we must still use a simpler model than the method would allow for. These simplifications should not be considered as restrictions of the method itself. As more information becomes available in the future, the method can be improved with ease to accommodate new information. In spite of the simplifications, the results we obtain provide in-

 ©1981 The American Physical Society

sight into how the various parameters in previous theories are connected and into how the band structure influences the impact ionization rate. In particular, the method is applied to study the electron-initiated ionization in GaAs. The results also give us information about the accuracy of the pseudopotential band structure at high energies.

II. SUMMARY OF EXPERIMENTAL RESULTS

Before we discuss the theory of impact ionization, it is instructive to summarize the available experimental data. Various experimental techniques to measure the ionization rate are described in detail in the review paper by Stillman and Wolfe.[1] Their article also contains some of the experimental data on the electron-initiated ionization rate in GaAs. Figure 1 summarizes more recent data.[16–19] The experimental results usually show a $1/F^2$ dependence of the ionization rate (F is the electric field). As can be seen from the figure, the data of different workers scatter almost by an order of magnitude.

Of special interest are the results of Pearsall *et al.*,[19] who measured the electron ionization rate with the electric field applied in three different crystallographic directions. Their data are replotted in Fig. 2. They have measured the highest ionization rate in the ⟨110⟩ direction and the lowest in the ⟨111⟩ direction. They have attributed this difference to ballistic electrons and electron trunneling to the next higher conduction band.[19,20] Although these data raise an interesting question as to how the band structure actually influences the ionization rate, their notion of ballistic electrons seems to be incorrect, as is shown in this work. More systematic and reliable data are necessary to make a comparison with the theory.

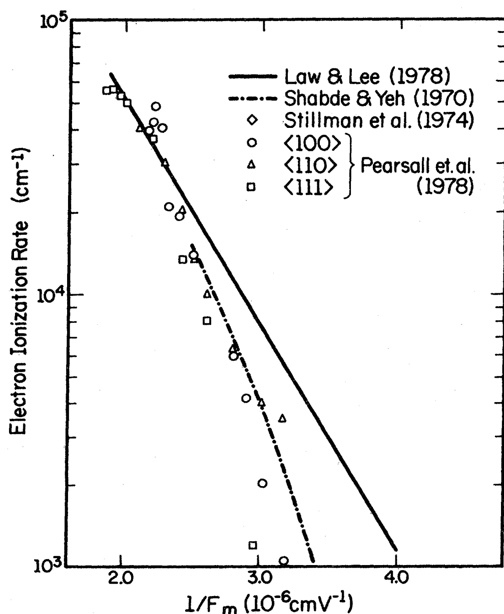

FIG. 1. Experimental ionization rates of electrons for GaAs at room temperature (Refs. 16–19).

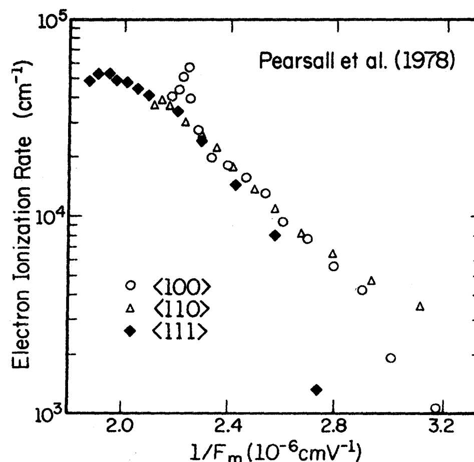

FIG. 2. Experimental electron ionization rates by Pearsall *et al.* (Ref. 19) as a function of reciprocal electric field for three orientations of electric field.

III. PREVIOUS THEORIES OF IMPACT IONIZATION

Wolff[3] was the first to calculate the ionization rate in semiconductors. He applied the gas discharge theory to solve the Boltzmann equation taking into account the effect of electron-phonon and pair-producing collisions on the distribution function. The velocity distribution function was approximated as

$$n(v,\theta)=n_0(v)+n_1(v)\cos\theta \ , \tag{1}$$

where v is the electron velocity, and θ is the angle between the velocity and the electric field. This is an energy diffusion theory, in which the electrons undergo many collisions when moving to higher energies. The Boltzmann equation was then solved to calculate the ionization rate with the result

$$\alpha(F)\sim\exp(-A/F^2) \ , \tag{2}$$

where F is the electric field.

Shockley,[4] on the other hand, argued that ionization is mainly due to "lucky" electrons which completely escape phonon scatterings and reach the threshold energy. In this streaming approximation the distribution is a spike in the direction of the electric field. He considered the relative probability of

phonon scattering and pair production, and obtained an ionization rate whose dependence on F is given by

$$\alpha(F) \sim \exp(-B/F) \ . \tag{3}$$

Next, Baraff[5,21] solve the time-independent Boltzmann equation and showed that his result contained Shockley's result as a low-field limit, and Wolff's result as a high-field limit. His theory gives the "universal" curves with phonon mean free path and ionization threshold energy as parameters, which are adjusted to fit theory to experimental data. However, it does not provide a way to calculate these quantities, nor does it include the band structure.

Recently, Chwang *et al.*[8] took a different approach using a finite Markov chain formation. Their method is based on the calculation of a transition matrix which characterizes the transition probability between virtual states defined by small discrete energy intervals. Interesting as it is, their method is limited by the analytical formulations. It still requires the same assumptions as Baraff's theory and does not produce much more information. For example, an assumption of a constant mean free path for phonon scattering is still necessary. Moreover, the Markov formulation is only applicable to nonpolar semiconductors.

Nevertheless, Baraff's and Chwang's theories contain some "truth" about the impact ionization mechanism, as does Shockley's and Wolff's approach. How they are related, and how they complement each other will be clear as a result of the Monte Carlo calculation described in this work. This Monte Carlo method includes a realistic band structure. As a result, the orientation dependence of the impact ionization can also be calculated.

IV. BAND STRUCTURE OF GaAs

The band structure of GaAs has been calculated using the empirical pseudopotential method as described by Cohen and Bergstresser.[15] Only the lowest conduction band has been considered. The effect of higher bands is briefly discussed in the later sections. Advantage is taken of the 48-fold symmetry of the Brillouin zone of the zinc-blende structure.[22] It is only necessary to examine a $\frac{1}{48}$th of the zone. This region is defined by the conditions

$$0 \leq k_z \leq k_x \leq k_y \leq 1 \tag{4}$$

and

$$k_x + k_y + k_z \leq \tfrac{3}{2} \ , \tag{5}$$

where all the k components are in units of $2\pi/a$ (a is the lattice constant, $a = 5.64$ Å for GaAs). Mesh points (k_x, k_y, $k_z = 0.0, 0.1, \ldots,$) are sampled from this region, and the energy and its gradient (velocity) at each k point are calculated. A total of 249 points have been sampled with 156 points within the region. The extra 93 points outside the region are necessary

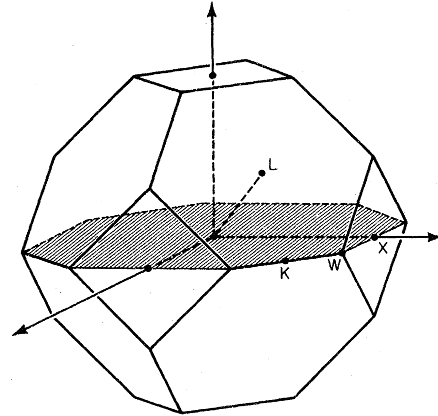

FIG. 3. Cross section of the Brillouin zone.

for the interpolation of energy in the proximity of the surface of the sampling region. Figure 4 illustrates the isoenergy lines in the cross section of the Brillouin zone shown in Fig. 3, with the numbers representing the electron energy from the bottom of the conduction band (at Γ). It can be seen that the Γ valley is nearly isotropic, whereas the X valleys are more elliptic. The band structure is then stored in memory, and used in the Monte Carlo simulation which is described in Sec. VI.

For the study of "lucky electron" transport extra $\vec{k}$ points have been sampled in three major crystal directions, i.e., the ⟨100⟩, ⟨110⟩, and ⟨111⟩ directions. The results have made it obvious (see, for example, Fig. 5 of Ref. 15) that the use of the effective mass and nonparabolicity is not valid for electron energies above approximately 1 eV in some directions. In fact, the effective mass defined as

$$\frac{1}{m^*} = \frac{1}{\hbar^2} \frac{\partial^2 E(k)}{\partial k^2} \tag{6}$$

goes to negative values at higher energies.

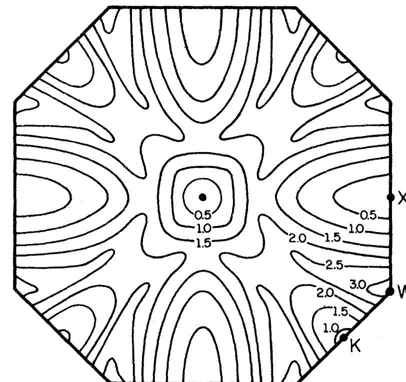

FIG. 4. Isoenergy lines of the lowest conduction band of GaAs in the cross section shown in Fig. 3. The numbers represent the energies measured from the Γ minimum.

V. BALLISTIC ELECTRON TRANSPORT AND PHONON SCATTERING

The term "ballistic electrons" has recently been used to denote those electrons which do not suffer phonon scattering.[20,23] This is equivalent to the "lucky" electron notion in Shockley's theory. Since the possible contribution of ballistic electrons to impact ionization has been suggested,[20] the behavior of ballistic electrons has been examined using the pseudopotential band structure. The study has been performed by solving the equations of motion

$$\hbar \frac{d\vec{k}}{dt} = e\vec{F} \tag{7}$$

and

$$\vec{v} = \frac{1}{\hbar} \vec{\nabla}_k E(\vec{k}) \ , \tag{8}$$

where $\vec{F}$ is the applied electric field, $\vec{k}$ is the electron wave vector, E is the electron energy, and $\vec{v}$ is the group velocity of the electron. Equations (7) and (8) are solved simultaneously with the initial condition $\vec{k}=\vec{0}$ at $t=0$, to express $\vec{v}$ and E as a function of time t. The field is assumed to be constant. Results of the calculations are shown in Fig. 5 for the three major crystallographic directions. The electric field has been chosen to be 500 kV/cm, a typical field for impact ionization. Figure 5 shows the electron velocity, $\vec{v}$, as a function of time. The orientation dependence of the ballistic behavior is obvious from this figure. The highest peak velocity is reached in the ⟨100⟩ direction ($\sim 1.1 \times 10^8$ cm/sec) and the lowest in the ⟨111⟩ direction ($\sim 0.8 \times 10^8$ cm/sec).

In a nonideal crystal, however, ballistic transport must compete with scattering processes. It will be shown by the Monte Carlo simulation that on the average an electron can travel ballistically for only $\sim 3 \times 10^{-14}$ sec before it suffers a phonon scattering. In the ⟨111⟩ direction, the electron can never gain sufficient energy ballistically for impact ionization.[19] In the ⟨100⟩ direction, the impact ionization threshold can be reached only if electrons tunnel in $\vec{k}$ space to the next higher band ~ 0.2 eV above the principal conduction band.[18,19] Therefore scattering events be-

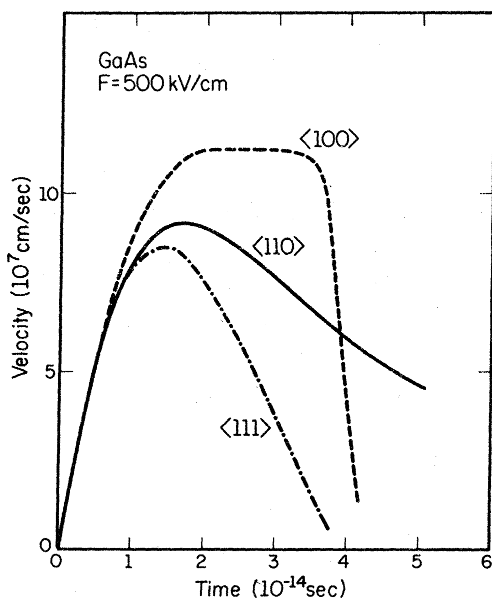

FIG. 5. Variation of ballistic electron velocity with time in three crystallographic directions of GaAs.

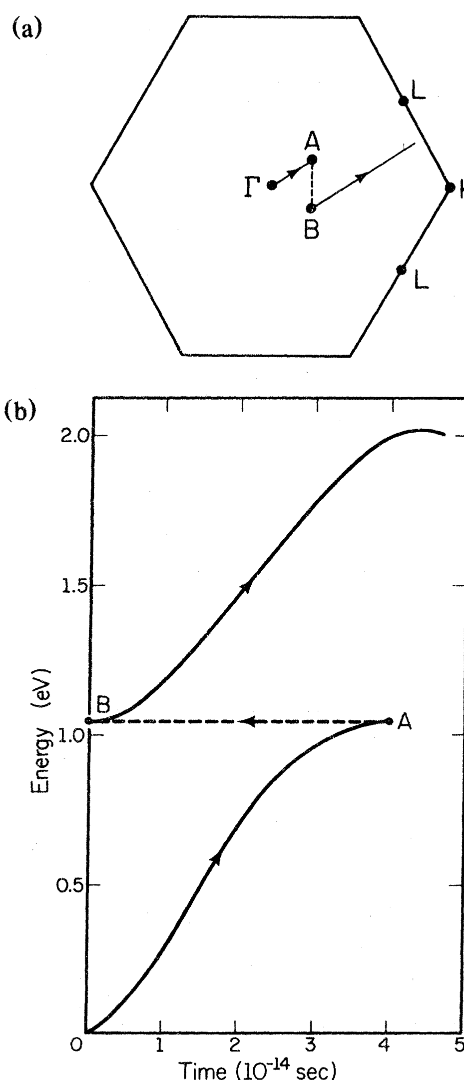

FIG. 6. (a) Example of wave-vector trajectory of electron in ΓKL plane under the influence of electric field in the ⟨111⟩ direction. Electron is scattered from A to B. Energy change in the scattering process has been neglected. (b) Variation with time of electron energy for the process shown in (a).

come crucial for the occurrence of impact ionization in these directions.

Electrons can be scattered to other regions of the Brillouin zone with a single scattering event being sufficient to permit the electrons to reach threshold energy. This mechanism is illustrated in Fig. 6 for an electric field applied in the ⟨111⟩ direction. An electron starts at the Γ point and moves along the ⟨111⟩ direction. At point $A\,[\vec{k}=(\pi/a)(0.3,0.3,0.3)]$, the energy is at the maximum for this direction, but it is still much less than the threshold energy. Subsequently, the electron can be scattered (by a phonon or impurity) to some other point in the Brillouin zone, point B, for example. Following this scattering event, the ⟨111⟩ component of the electron wave vector continues to increase. However, the wave vector points in a direction different from the ⟨111⟩ so that the electron can now reach a higher energy. As shown in Fig. 6, the electron can actually exceed the threshold energy for impact ionization ($\sim$2.0 eV).

This is, of course, only one example of an electron trajectory to show the importance of scattering processes to impact ionization. The actual calculation of the impact ionization rate must involve averaging of all the possible electron trajectories until the electron reaches the threshold energy. This is achieved by the Monte Carlo method which is described in the next section.

VI. SIMULATION METHOD

The Monte Carlo simulation keeps track of an electron $\vec{k}$ vector in the Brillouin zone until it reaches the threshold energy for impact ionization. This is done with a knowledge of scattering mechanisms, scattering rates, and band structure in the whole Brillouin zone. The $E(\vec{k})$ relation for an arbitrary $\vec{k}$ point can be calculated in the following way. First, the $\vec{k}$ point is mapped into the sampling region by using the point-group symmetry. The energy is then calculated by quadratic interpolation utilizing the energies and the gradients of the surrounding eight mesh points. The gradient is interpolated only linearly. Applying the inverse operations on the calculated energy and gradient gives the $E(\vec{k})$ relation and the gradient at the original $\vec{k}$ point.

Next we need to know the phonon scattering rate. Ideally the scattering rate should be calculated at each $\vec{k}$ point in order to take into account the overlap integral.[24] Also, when the initial or final electron state is not on the symmetry points, the selection rules[25] become less restrictive and this may give rise to additional scattering. Moreover, even near the bottom of the valleys, it is known that the scattering rates are different in the Γ, L, and X valleys. We have assumed the scattering rate to be isotropic (only energy dependent) for simplicity and because of lack of additional information. We have taken the scattering rate as given for the central valley. This overestimates the scattering rate when the electron is in the satellite valleys. The simplification is partly justified by the fact that the scattering rates of different valleys approach each other at higher energies. Furthermore, since scattering to upper bands is possible in reality (which increases the scattering rate in the satellite valleys), the overestimation is at least partly compensated.

The values of the parameters for the calculation of the scattering rate are the same as the ones used in the simulation of the Gunn effect.[26] They are known to give a good fit to the experimental data at low fields. Below 0.33 eV only polar optical scattering occurs in the central valley. Above 0.33 eV polar optical scattering occurs only when an electron is in the central valley arbitrarily defined as

$$-0.3 \leq k_x,\ k_y,\ k_z \leq 0.3 \ , \tag{9}$$

where the components are in units of $2\pi/a$. Otherwise intervalley scattering occurs. It is not appropriate to simply extend the scattering rate to higher energies because of the complicated band structure. Because the intervalley scattering rate is proportional to the density of final states, and the density of states in the conduction band decreases nearly quadratically above 1.5 eV,[27] we have assumed a quadratically decreasing scattering rate above 1.5 eV. The resultant total scattering rate as a function of electron energy is shown in Fig. 7 (solid line). The maximum scattering rate is $4.5\times10^{14}\ \mathrm{sec}^{-1}$ at 1.5 eV.

In the ⟨100⟩ direction the threshold state for electron-initiated ionization lies in the second conduction band.[18] An electron can tunnel through the "pseudogap" ($\sim$0.2 eV) between the lowest and the second conduction band to reach threshold. No attempt has been made to simulate this tunneling mechanism. Since the tunneling time is estimated to be of the order of 1×10^{-13} sec,[18] and the intervalley scattering time for an electron energy of 2.0 eV is much shorter ($<1\times10^{-14}$ sec) than this tunneling time, electrons are more likely to be scattered before they can tunnel to the upper band. Therefore, the contribution of these tunneling electrons to impact ionization is expected to be small.

The final state of the scattering process is determined in the following way. Since polar optical scattering is dominant only at low energies in the central valley, the usual formula with effective mass and nonparabolicity terms is used to choose a candidate for the final $\vec{k}$ point. The energy at this $\vec{k}$ point is then recalculated using the exact band structure to check if it is within an allowed range (typically 30 meV) around the final energy (for example, $E+\hbar\omega_0$ in the case of phonon absorption). If it is outside this range, a different final state is chosen and the process is repeated until a proper state within the correct energy range is found. Intervalley scattering

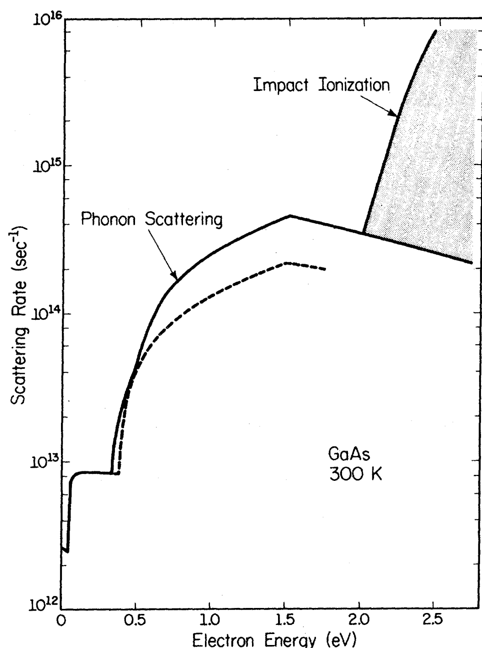

FIG. 7. Phonon scattering rate and the impact ionization probability in GaAs as a function of electron energy. The parameters are due to Littlejohn *et al.* (solid line) (Ref. 26) and Vinson *et al.* (broken line) (Ref. 33).

is known to be completely randomizing.[28] For this mechanism, once the final energy is calculated, those mesh points whose energies are within the allowed range are tabulated. One of them is then randomly selected as the final state. The correct overall energy loss is checked and ensured in our procedure.

Our treatment of phonon scattering processes represents a compromise between accuracy and numerical tractability. For a finite number of mesh points, the energy separation between any two $\vec{k}$ points is finite. For example, for our 156 mesh points this energy separation can be as large as 60 meV. The allowed energy range during the scattering must be large enough to bridge this gap in order to assure the continuity of the energy band. In the limit of infinitely fine mesh points, the allowed range for final energy can be infinitely small. The number of $\vec{k}$ points in this energy range for a given final energy is proportional to the density of states at each region of $\vec{k}$ space with this final energy. Therefore, in the limit of infinitely fine mesh our procedure is correct, since the scattering rate for deformation potential scattering is proportional to the final density of states.

The impact ionizing collision is treated as an additional scattering mechanism. We assume an isotropic threshold energy of 2.0 eV. Anderson and Crowell[9] have shown that the threshold energy actually depends on the $\vec{k}$ vector. However, their graphical procedure is almost impossible to perform in three-dimensional momentum space. A more systematic approach may be possible.[29] If the threshold energy is calculated for each $\vec{k}$ point, it can be easily included in this simulation procedure. The impact ionization probability can be calculated from the matrix element for the screened Coulomb interaction.[14,30,31] However, here we use a simpler model demonstrated by Keldysh[6,32] and used by others.[8] According to Keldysh the probability of impact ionization can be represented as

$$\frac{1}{\tau_i(E)} = \frac{1}{\tau(E_i)} P \left(\frac{E - E_i}{E_i} \right)^2 , \tag{10}$$

where E is the electron energy, E_i is the threshold energy, $1/\tau(E_i)$ is the scattering rate at $E = E_i$, and P is a dimensionless constant which is usually much larger than unity. This formula is valid for semiconductors with large dielectric constants. We take P as a parameter. $P = \sim 50 - \infty$ has been used by Chwang *et al.*[8] As shown by Baraff,[5] and then by Chwang[8] the impact ionization rate does not strongly depend on this parameter as long as P is large compared to unity. The energy dependence of the impact ionization probability for $P = 400$ is illustrated in Fig. 7.

Once the scattering rate and the ionization probability are determined, the rest of the simulation procedure is similar to the conventional Monte Carlo method.[11] The scattering probability $[\Delta t/\tau(E)]$ is calculated at each time interval, Δt, and compared with a random number. This is necessary because of the complicated $E(\vec{k})$ relation. Δt is taken to be approximately $\frac{1}{10}$th the average drift time. The simulation starts by releasing an electron with zero energy at the bottom of the central valley. The energy and the $\vec{k}$ vector of the electron are traced. When impact ionization occurs, the energy is reinitialized to zero to start a new history. This is justified by the fact that the resultant electron after ionization lies very close to the bottom of the central valley.[9] The impact ionization rate can be obtained by averaging each distance that an electron travels until impact ionization occurs over a sufficient number of ionizations. The distance, Δx, traveled during each drift is calculated either by accumulating a differential distance, $v\Delta t$, or by utilizing the relation

$$\Delta E = eF\Delta x , \tag{11}$$

where ΔE is the energy gained during the drift. The velocity v is calculated from the gradient of the $E(\vec{k})$ relation.

VII. RESULTS

A. Contribution of ballistic electrons

By terminating the simulation after the first scattering the electron suffers, the behavior of ballistic elec-

trons can be studied. Additionally, we can determine the extent which these ballistic electrons contribute to impact ionization. Since there is no electron-initiated threshold state in the ⟨100⟩ or the ⟨111⟩ direction,[19] we only consider the ⟨110⟩ direction. We have also changed the threshold energy to 1.7 eV, which is the correct threshold energy in this direction.[9] Typically 100 000 trials have been done for each electric field.

The result of the calculation shows that an electron travels on the average approximately 200 Å, for an average time of 3×10^{-14} sec before the first scattering event. These numbers differ slightly for different orientations. By counting those electrons which cause impact ionization instead of scattering, we can estimate the contribution of ballistic electrons to the impact ionization rate. If the same scattering rate is used as shown in Fig. 7 (known to give a good fit to the Gunn effect[26]), we find no electrons (less than 0.001%) causing impact ionization. There may be some uncertainties in the scattering rate, particularly in the values of the deformation potential constants. To find the maximum possible contribution of ballistic electrons to impact ionization, a smaller scattering rate has been tried. We have used the values given by Vinson *et al.*[33]: $E_{\Gamma-X}=0.4$, $E_{\Gamma-L}=0.38$ eV, $D_{\Gamma-X}=1.1\times10^9$, and $D_{\Gamma-L}=2.8\times10^8$ eV/cm. This gives the scattering rate shown by the broken line in Fig. 7. This rate is approximately half of the previous value. Using this scattering rate in our calculation we obtain the results shown in Fig. 8. This figure shows the probability that an electron causes impact ionization prior to its scattering by a phonon as a function of electric field. As can be seen, even at the maximum (500 kV/cm for $P=\infty$), only 0.2% of the electrons causing impact ionization are "ballistic." Therefore we conclude that the contribution of ballistic electrons to impact ionization is negligibly small if our present understanding of the scattering rate is correct. This conclusion negates the considerations by Capasso *et al.*[20] who suggested that ballistic electrons give a non-negligible contribution to the total ionization rate.

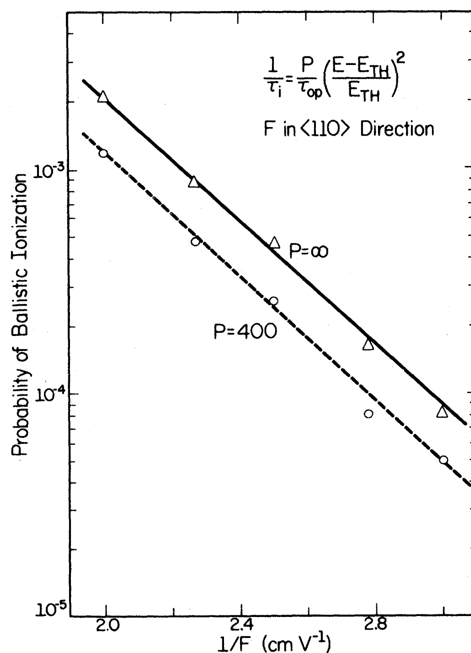

FIG. 8. Probability of ballistic electron causing impact ionization as a function of a reciprocal electric field.

These "ballistic" electrons were discussed by Shockley who called them "lucky" electrons.[4] We have shown that Shockley's theory gives ionization rates that are too small. It is interesting to note, however, that the two curves in Fig. 8 show the correct $1/F$ dependence as in Shockley's theory in spite of the much more complicated band structure and scattering rate that we used.

B. Transport properties and ionization rate

In the calculation of the impact ionization rate a typical simulation consists of approximately 200 000 to 400 000 scattering events. Depending on electric field this would give 40–300 impact ionization events. Figure 9 shows a typical trajectory of the $\vec{k}$ vector in the Brillouin zone for an electric field of 500 kV/cm in the ⟨100⟩ direction. The solid lines represent the drift of the electron, and the broken lines represent the scatterings from one end to the next. When the $\vec{k}$ comes to lie outside of the Brillouin zone, it is placed back inside the zone to the equivalent point. This is done by adding the appropri-

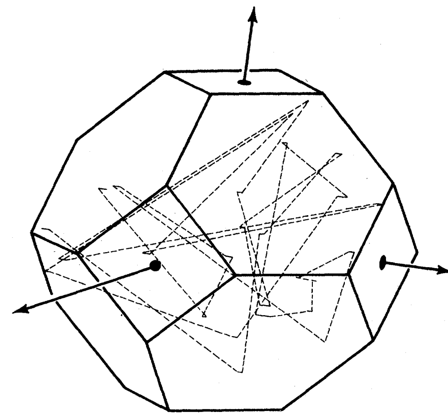

FIG. 9. Typical trajectory of the electron $\vec{k}$ vector in the Brillouin zone for an electric field of 500 kV/cm. The solid lines represent the drift and the broken lines represent the scatterings from one point to the next.

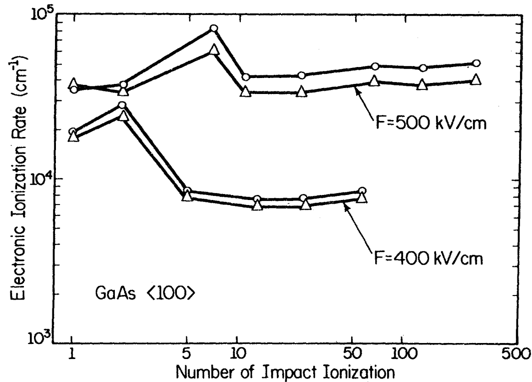

FIG. 10. Impact ionization rate in GaAs as a function of the number of ionizations obtained with the Monte Carlo simulation. The calculation is from the slope of the $E(\vec{k})$ curve (Δ) or from Eq. (11) ($\circ$).

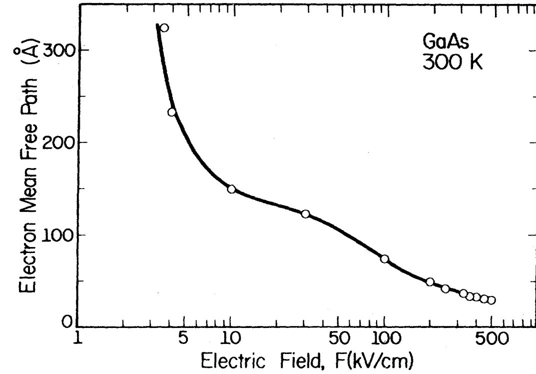

FIG. 12. Electron mean free path in GaAs as a function of electric field calculated by the Monte Carlo simulation (steady state).

ate reciprocal-lattice vector to the original $\vec{k}$ vector. As seen from the figure the drift time is very short because of the high scattering rate at higher energies. The electron is frequently scattered over practically the entire Brillouin zone.

Figure 10 shows how the calculated ionization rate converges as the number of ionizations is increased. Because of the limited computer time it has not been possible to take averages over more than 300 ionizations. However, the convergence is fairly good after 10 ionizations. From this figure the statistical fluctuation is estimated to be approximately 20%. The problem of statistical fluctuation can be overcome by repeating the simulation only for the high-energy tail.[34] This has not been attempted in this work.

Figure 11 shows the average electron energy as a function of the electric field. The reason for the steeper increase beyond 100 kV/cm is not understood, but may be related to the band structure. Figure 12 shows the electron mean free path as a function of electric field. In the electric field range where impact ionization occurs, the mean free path between phonon scattering ranges from 50 to 30 Å. This is in agreement with previous data[2,35] and the conventional Monte Carlo calculation.[10] The reason that our calculation agrees in this respect with the conventional interpretation which does not include a realistic band structure is that the mean free path is mainly determined by the average electron energy, which is still small enough ($\sim$0.8 eV) for effective mass and nonparabolicity corrections to be sufficient (at least in certain $\vec{k}$ directions).

The calculated electric field dependence of the electron drift velocity is shown in Fig. 13. The broken curve represents the experimental data by Ruch and Kino[36] at low electric field ($<$14 kV/cm), and by Houston and Evans[37] at high field ($\sim$20–100 kV/cm). The agreement is good over the entire range of electric fields experimentally investigated. The result using Eq. (11) gives much better fit than the result using the slopes of the $E(\vec{k})$ relation. It is

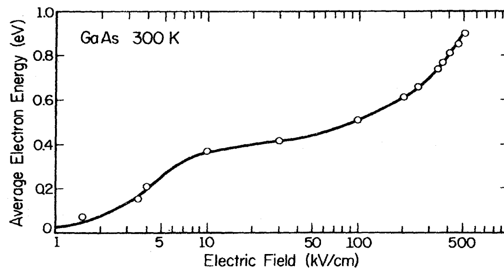

FIG. 11. Average electron energy in GaAs as a function of electron field calculated by the Monte Carlo simulation.

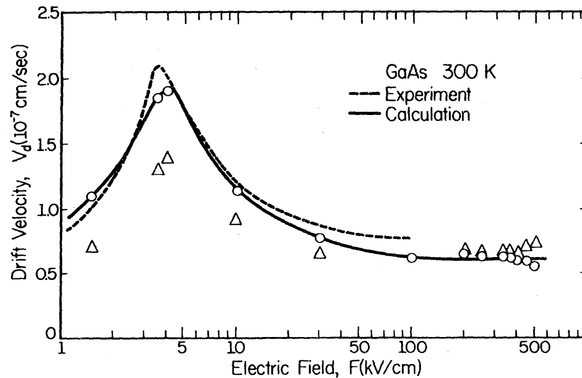

FIG. 13. Calculated electron drift velocity in GaAs at room temperature compared with the experimental data (Refs. 36 and 37). The calculated values are from the slope of the $E(\vec{k})$ curve (Δ) or from Eq. (11) ($\circ$).

suspected that the accumulation of numerical errors in the slope calculation is responsible for the discrepancy. The slight deviations between theory and experiment at higher fields are believed to be mainly due to the pseudopotential band structure which gives the satellite valley effective masses larger than are usually assumed. From Fig. 13 it can also be seen that the calculations describe quantitatively the Gunn effect. This means that the method can simulate polar optical scattering as well as intervalley scattering, and that the transition from polar optical scattering (low-energy region) to intervalley scattering (high-energy region) is accomplished smoothly.

Figure 14 shows the calculated electric field dependence of the impact ionization rate in GaAs for three different crystal orientations. We have assumed $P = 400$. The shaded region indicates the range covered by the experimental data (Sec. II). The agreement is fair, considering the uncertainty in the scattering rate at higher energies. The inclusion of upper bands is expected to increase the calculated ionization rate slightly, and therefore to improve the fit to the experimental data. Note, however, that the calculation shows within statistical uncertainty ($\sim 20\%$) no orientation dependence for the ionization rate. This contradicts previous interpretations of the experimental data by Pearsall *et al.*[19] (Fig. 2). Another way to calculate the orientation dependence is rotating the electric field direction from one axis to another. The result is shown in Fig. 15 for an electric field of 400 kV/cm when the field is rotated from the $\langle 110 \rangle$ to $\langle 111 \rangle$ direction. Again we do not see

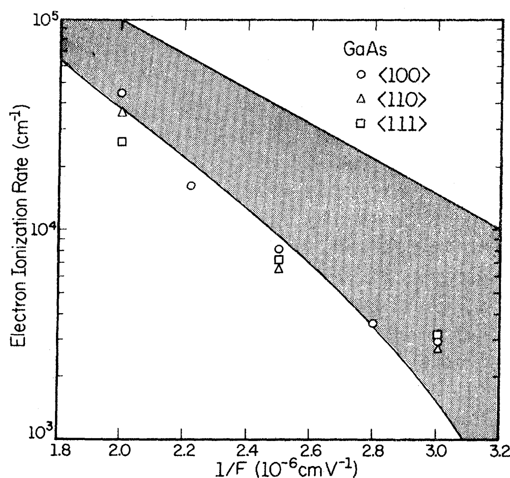

FIG. 14. Calculated impact ionization rate of an electron in GaAs with an electric field in three crystallographic directions as a function of a reciprocal field. The shaded region indicates the range of available experimental data (Fig. 1). Within statistical uncertainty, we do not observe any orientation dependence.

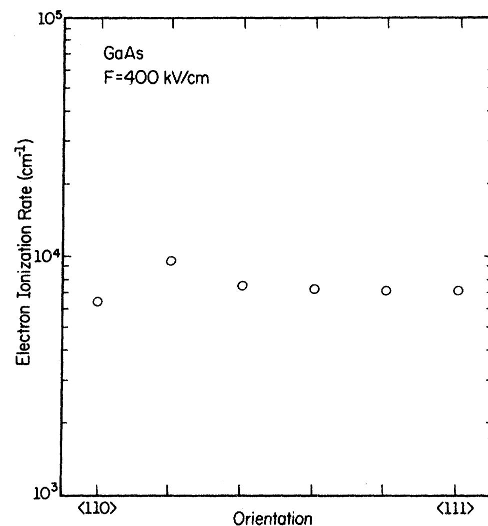

FIG. 15. Calculated impact ionization rate of an electron with an electric field of 400 kV/cm in several directions between the $\langle 110 \rangle$ and $\langle 111 \rangle$ directions.

any orientation dependence within the statistical uncertainty. A solution including this rotation of the electric field can be obtained only by the Monte Carlo method. The effect of changing the value of P has also been examined. Varying P from 50 to 400 we have obtained practically the same impact ionization rate. This confirms the result by Baraff[5] and Chwang[8] that the ionization rate is insensitive to the ionization probability as long as it is much larger than the probability of phonon scattering.

For a better understanding of how the electrons acquire the high energies, and how impact ionization is actually accomplished, we show in Figs. 16 and 17 the variation of electron energy after each scattering event for electric fields of 500 and 100 kV/cm, respectively. In the case of 500 kV/cm, the electron energy stays around $\sim 0.7-1.2$ eV most of the time, but the electron occasionally escapes phonon scattering and moves up to higher energies. In Fig. 16 we can see $\sim 4-5$ spikes which reach to ~ 1.8 eV. When an electron reaches 2.0 eV, it causes impact ionization. We can think of these electrons as the "lucky electrons" in Shockley's theory, and those electrons around the average energy as the diffusing (in energy) electrons in Wolff's theory. However, as seen in the figure this classification is not very distinct. Even those electrons in the spikes suffer several scatterings before they reach the peak energies. Our results, therefore, contain Shockley's and Wolff's notions of ionizing electrons as does Baraff's theory (but we have much more general conditions). Using Baraff's word,[5] the notion of ballistic electrons by Shockley and diffusing electrons by Wolff are "complementary" in

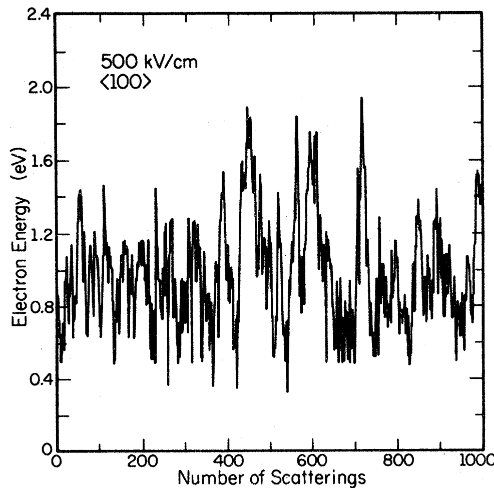

FIG. 16. Variation of electron energy after each scattering event for an electric field of 500 kV/cm obtained with a Monte Carlo simulation.

determining the impact ionization rate. This is due to the fact that the height of spikes (in Fig. 16) depends on the average energy of electrons. It is also important to note the difference between our ionizing electrons and Shockley's "lucky" electrons. Shockley's "lucky" electrons start from zero energy, escape the phonon scattering completely, and impact ionize. The ionizing electrons of our result start at the average energy and reach ionization threshold after a few scattering events. This explains why Shockley's theory badly underestimates the ionization rate, since he neglected electrons which are scattered at intermediate energy.

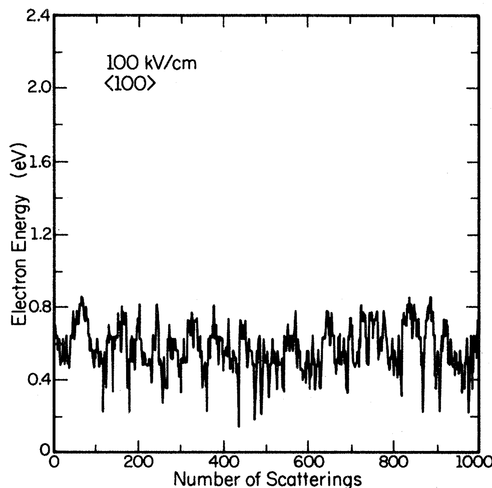

FIG. 17. Variation of electron energy after each scattering event for an electric field of 100 kV/cm.

VIII. CONCLUSIONS

A Monte Carlo simulation of high-field transport in GaAs employing a realistic band structure has been described. The method has been used to study the impact ionization mechanism in GaAs. The band structure of GaAs has been calculated using the empirical pseudopotential method. Partly due to lack of information and partly for simplicity, we have used simplifying assumptions for the phonon scattering rates, the ionization threshold energy, and the ionization probability. This, however, is not an inherent limitation of the method. Unlike previous theories of impact ionization, the method requires, in principle, no adjustable parameters as long as the band structure and the scattering mechanism are known. The method has provided new results and increased the understanding of high-field transport and impact ionization in GaAs. The calculated drift velocity, the mean free path, and the impact ionization rate are in fair agreement with some of the published experimental data. The inclusion of the higher conduction bands is expected to further improve the fit. We do not expect, however, to obtain the anisotropy measured by Pearsall *et al.*[19] In our opinion this anisotropy is not a consequence of the band structure, but is rather caused by crystal defects or other effects not yet understood. It is found that the contribution of ballistic electrons to the impact ionization rate is negligibly small. Shockley's theory, therefore, badly underestimates the ionization rate. We have confirmed that the impact ionization rate is rather insensitive to the ionization probability above the threshold energy as long as the probability is much larger than the phonon scattering rate.

Based on the results of the simulation, a general discussion of impact ionization has been given. We find that typically electrons stay around an average energy and experience a large number of phonon scatterings. Occasionally electrons escape phonon scattering and move up to higher energy. Some reach ionization threshold after a few scattering events. This feature is seen in Fig. 16. It can be considered as a combination of Wolff's and Shockley's notion of ionizing electrons, but the distinction is rather vague. The reason for the success of Baraff's theory is that his theory also contains this feature. However, because of his formulation using distribution functions, the physical picture is not as clear as in our result (Fig. 16). Moreover, our method includes realistic scattering mechanisms and band structure.

Unlike previous theories of impact ionization, the present method can in principle be applied to any semiconductor. The method can be used for both polar and nonpolar materials. This is obvious from the successful simulation of the Gunn effect, which

contains the transition from polar optical scattering to intervalley scattering. The calculation of hole-initiated ionization rates should also be possible, although presently our understanding of hole transport is not as deep as electron transport. This is important for the understanding of the operation of photodetectors, since their performance depends on the ratio of electron- and hole-initiated ionization rates. It should be understood that the method is quite versatile in its application. A transient Monte Carlo method including the band structure may be used to investigate the orientation dependence of the avalanche response time.[38] Finally the inclusion of the position dependence should enable us to study the effect of the "dark space."[39]

ACKNOWLEDGMENTS

The authors wish to thank E. M. Kesler, R. T. Gladin, and R. F. MacFarlane for technical assistance. They are grateful to Professor G. E. Stillman, Professor B. G. Streetman, and Professor N. Holonyak, Jr., for many valuable discussions. The use of the computer facilities of the Materials Research Laboratory, University of Illinois, is also gratefully acknowledged. The work was supported by the Office of Naval Research and the Joint Services Electronics Program.

---

[1]G. E. Stillman and C. M. Wolfe, in *Semiconductors and Semimetals,* edited by R. K. Willardson and A. C. Beers (Academic, New York, 1977), Vol. 12.

[2]S. M. Sze, *Physics of Semiconductor Devices* (Wiley, New York, 1969).

[3]P. A. Wolff, Phys. Rev. 95, 1415 (1954).

[4]W. Shockley, Solid State Electron. 2, 35 (1961).

[5]G. A. Baraff, Phys. Rev. 128, 2507 (1962).

[6]L. V. Keldysh, Sov. Phys. JETP 21, 1135 (1965).

[7]W. P. Dumke, Phys. Rev. 167, 783 (1968).

[8]R. Chwang, C. W. Kao, and C. R. Crowell, Solid State Electron. 22, 599 (1979).

[9]C. L. Anderson and C. R. Crowell, Phys. Rev. B 5, 2267 (1972).

[10]J. R. Hauser, Appl. Phys. Lett. 33, 351 (1978).

[11]W. Fawcett, A. D. Boardman, and S. Swain, J. Phys. Chem. Solids 31, 1963 (1970).

[12]P. J. Price, in *Semiconductors and Semimetals,* edited by R. K. Willardson and A. C. Beer (Academic, New York, 1979), Vol. 14.

[13]P. A. Lebwohl and P. J. Price, Solid State Commun. 9, 1221 (1971).

[14]R. C. Curby and D. K. Ferry, Phys. Status Solidi A 15, 319 (1973).

[15]M. L. Cohen and T. K. Bergstresser, Phys. Rev. 141, 789 (1966).

[16]S. N. Shabde and C. Yeh, J. Appl. Phys. 41, 4743 (1970).

[17]G. E. Stillman, C. M. Wolfe, J. A. Rossi, and A. G. Foyt, Appl. Phys. Lett. 24, 471 (1974).

[18]H. D. Law and C. A. Lee, Solid State Electron. 21, 331 (1978).

[19]T. P. Pearsall, F. Capasso, R. E. Nahory, M. A. Pollack, and J. R. Chelikowsky, Solid State Electron. 21, 297 (1978).

[20]F. Capasso, R. E. Nahory, and M. A. Pollack, Solid State Electron. 22, 977 (1979).

[21]G. A. Baraff, Phys. Rev. 133, A26 (1964).

[22]D. Brust, Phys. Rev. 134, A1337 (1964).

[23]M. S. Shur and L. F. Eastman, IEEE Trans. Electron Devices ED-26, 1677 (1979).

[24]D. Matz, Phys. Rev. 168, 843 (1968).

[25]J. L. Birman, M. Lax, and R. Loudon, Phys. Rev. 145, 620 (1966).

[26]M. A. Littlejohn, J. R. Hauser, and T. H. Glisson, J. Appl. Phys. 48, 4587 (1977).

[27]J. R. Chelikowsky and M. L. Cohen, Phys. Rev. B 14, 556 (1976).

[28]E. M. Conwell, *Solid State Physics* (Academic, New York, 1967), Suppl. 9.

[29]P. T. Landsberg and D. J. Robbins, J. Phys. C 10, 2717 (1977).

[30]E. Antončík, Czech. J. Phys. B 17, 735 (1967).

[31]D. J. Robbins, Phys. Status Solidi B 97, 9 (1980).

[32]L. V. Keldysh, Sov. Phys. JETP 10, 509 (1960).

[33]P. J. Vinson, C. Pickering, A. R. Adams, W. Fawcett, and G. D. Pitt, in Proceedings of 23th International Conference on Physics of Semiconductors, Rome, 1976 (unpublished).

[34]P. J. Price (private communication).

[35]H. Kressel and G. Kupsky, Int. J. Electron. 20, 535 (1966).

[36]J. G. Ruch and G. S. Kino, Phys. Rev. 174, 921 (1968).

[37]P. A. Houston and A. G. R. Evans, Solid State Electron. 20, 197 (1977).

[38]J. J. Barenz, J. Kinoshita, T. L. Hierl, and C. A. Lee, Electron. Lett. 15, 150 (1979).

[39]Y. Okuto and C. R. Crowell, Phys. Rev. B 10, 4284 (1974).

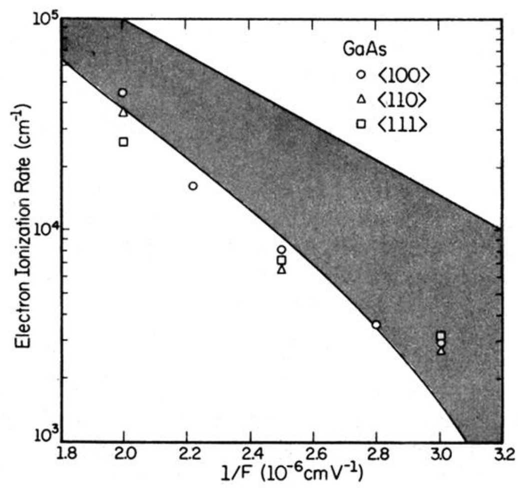

FIG. 14. Calculated impact ionization rate of an electron in GaAs with an electric field in three crystallographic directions as a function of a reciprocal field. The shaded region indicates the range of available experimental data (Fig. 1). Within statistical uncertainty, we do not observe any orientation dependence.

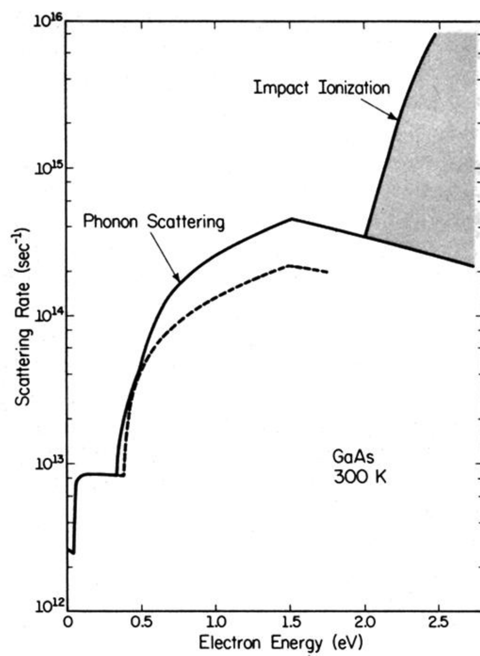

FIG. 7. Phonon scattering rate and the impact ionization probability in GaAs as a function of electron energy. The parameters are due to Littlejohn *et al.* (solid line) (Ref. 26) and Vinson *et al.* (broken line) (Ref. 33).